



HAL
open science

Generation of ultrahigh and tunable repetition rates in CW injection-seeded frequency-shifted feedback lasers

Hugues Guillet de Chatellus, Olivier Jacquin, Olivier Hugon, Wilfried Glastre, Eric Lacot, Jens Marklof

► **To cite this version:**

Hugues Guillet de Chatellus, Olivier Jacquin, Olivier Hugon, Wilfried Glastre, Eric Lacot, et al.. Generation of ultrahigh and tunable repetition rates in CW injection-seeded frequency-shifted feedback lasers. *Optics Express*, 2013, 21 (issue 13), pp.15065-15074. 10.1364/OE.21.015065 . hal-00951911

HAL Id: hal-00951911

<https://hal.science/hal-00951911>

Submitted on 27 Feb 2014

HAL is a multi-disciplinary open access archive for the deposit and dissemination of scientific research documents, whether they are published or not. The documents may come from teaching and research institutions in France or abroad, or from public or private research centers.

L'archive ouverte pluridisciplinaire **HAL**, est destinée au dépôt et à la diffusion de documents scientifiques de niveau recherche, publiés ou non, émanant des établissements d'enseignement et de recherche français ou étrangers, des laboratoires publics ou privés.

Generation of ultrahigh and tunable repetition rates in CW injection-seeded frequency-shifted feedback lasers

H. Guillet de Chatellus,^{1,*} O. Jacquin,¹ O. Hugon,¹ W. Glastre,¹
E. Lacot,¹ and J. Marklof²

¹CNRS/Univ. Grenoble I, Laboratoire Interdisciplinaire de Physique, UMR 5588, Grenoble, F-38041, France

²School of Mathematics, University of Bristol, Bristol BS8 1TW, UK

[*hugues.guilletdechatellus@ujf-grenoble.fr](mailto:hugues.guilletdechatellus@ujf-grenoble.fr)

Abstract: We show both theoretically and experimentally that frequency-shifted feedback (FSF) lasers seeded with a single frequency laser can generate Fourier transform-limited pulses with a repetition rate tunable and limited by the spectral bandwidth of the laser. We demonstrate experimentally in a FSF laser with a 150 GHz spectral bandwidth, the generation of 6 ps-duration pulses at repetition rates tunable over more than two orders of magnitude between 0.24 and 37 GHz, by steps of 80 MHz. A simple linear analytical model *i.e.* ignoring both dynamic and non-linear effects, is sufficient to account for the experimental results. This possibility opens new perspectives for various applications where lasers with ultra-high repetition rates are required, from THz generation to ultrafast data processing systems.

© 2013 Optical Society of America

OCIS codes: (030.4070) Modes; (140.3538) Lasers, pulsed; (140.4050) Mode-locked lasers.

References and links

1. M. Stellpflug, G. Bonnet, B. W. Shore, and K. Bergmann, "Dynamics of frequency shifted feedback lasers: simulation studies," *Opt. Express* **11**, 2060–2080 (2003).
2. F. V. Kowalski, C. Ndiaye, K. Nakamura, and H. Ito, "Noise waveforms with repetitive phase and nonrepetitive amplitude," *Opt. Lett.* **27**, 1965–1967 (2002).
3. L. P. Yatsenko, B. W. Shore, and K. Bergmann, "Coherence in the output spectrum of frequency shifted feedback lasers," *Opt. Commun.* **282**, 300–309 (2009).
4. H. Guillet de Chatellus and J.-P. Pique, "Statistical properties of frequency shifted feedback lasers," *Opt. Commun.* **283**, 71–77 (2010).
5. F. V. Kowalski, C. Ndiaye, K. Nakamura, and H. Ito, "Noise waveforms generated by frequency shifted feedback lasers: application to multiple access communications," *Opt. Commun.* **231**, 149–164 (2004).
6. H. Guillet de Chatellus and J.-P. Pique, " $\lambda/2$ fringe spacing interferometer," *Opt. Lett.* **34**, 755–757 (2009).
7. K. Nakamura, T. Hara, M. Yoshida, T. Miyahara, and H. Ito, "Optical frequency domain ranging by a frequency-shifted feedback laser," *IEEE J. Quantum Electron.* **36**, 305–316 (2000).
8. V. V. Ogurtsov, L. P. Yatsenko, V. M. Khodakovskyy, B. W. Shore, G. Bonnet, and K. Bergmann, "High accuracy ranging with Yb³⁺-doped fiber-ring frequency-shifted feedback laser with phase-modulated seed," *Opt. Commun.* **266**, 266–273 (2006).
9. H. Guillet de Chatellus, E. Lacot, W. Glastre, O. Jacquin, and O. Hugon, "The hypothesis of the moving comb in frequency shifted feedback lasers," *Opt. Commun.* **284**, 4965–4970 (2011).
10. H. Guillet de Chatellus, E. Lacot, O. Jacquin, W. Glastre, and O. Hugon, "Heterodyne beatings between frequency-shifted feedback lasers," *Opt. Lett.* **37**, 791–793 (2012).
11. S. Balle, I. C. Littler, K. Bergmann, and F. V. Kowalski, "Frequency shifted feedback dye laser operating at a small shift frequency," *Opt. Commun.* **102**, 166–173 (1993).

12. F. V. Kowalski, S. J. Shattil, and P. D. Hale, "Optical pulse generation with a frequency shifted feedback laser," *Appl. Phys. Lett.* **53**(9), 734–736 (1988).
13. H. Sabert and E. Brinkmeyer, "Pulse generation in fiber lasers with frequency shifted feedback," *J. Lightwave Technol.* **12**, 1360–1368 (1994).
14. G. Bonnet, S. Balle, T. Kraft, and K. Bergmann, "Dynamics and self-modelocking of a titanium-sapphire laser with intracavity frequency shifted feedback," *Opt. Commun.* **123**, 790–800 (1996).
15. J. M. Sousa and O. G. Okhotnikov, "Short pulse generation and control in Er-doped frequency-shifted-feedback fiber lasers," *Opt. Commun.* **183**, 227–241 (2000).
16. M. P. Nikodem, H. Sergeant, P. Kaczmarek, and K. M. Abramski, "Actively mode-locked fiber laser using acousto-optic modulator," *Proc. SPIE* **7141**, 71410B (2008).
17. M. P. Nikodem, E. Kluzniak, and K. Abramski, "Wavelength tunability and pulse duration control in frequency shifted feedback Er-doped fiber lasers," *Opt. Express* **17**, 3299–3304 (2009).
18. A. M. Heidt, J. P. Burger, J.-N. Maran, and N. Traynor, "High power and high energy ultrashort pulse generation with a frequency shifted feedback fiber laser," *Opt Express* **15**, 15892–15897 (2007).
19. F. V. Kowalski, J. A. Squier, and J. T. Pinckney, "Pulse generation with an acousto-optic frequency shifter in a passive cavity," *Appl. Phys. Lett.* **50**, 711–713, 1987.
20. P. D. Hale and F. V. Kowalski, "Output characterization of a frequency shifted laser: Theory and experiment," *IEEE J. Quantum Electron.* **26**, 1845–1851 (1990).
21. M. W. Phillips, G. Y. Liang, and J. R. M. Barr, "Frequency comb generation and pulsed operation in a Nd:YLF laser with frequency-shifted feedback," *Opt. Commun.* **100**, 473–478 (1993).
22. P. Coppin and T. G. Hodgkinson, "Novel optical frequency comb synthesis using optical feedback," *Electron. Lett.* **26**, 28–30 (1990).
23. L. P. Yatsenko, B. W. Shore, and K. Bergmann, "Theory of a frequency-shifted feedback laser," *Opt. Commun.* **236**, 183–202 (2004).
24. V. V. Ogurtsov, L. P. Yatsenko, V. M. Khodakovskyy, B. W. Shore, G. Bonnet, and K. Bergmann, "Experimental Characterization of an Yb³⁺-doped Fiber Ring Laser with Frequency-shifted Feedback," *Opt. Commun.* **266**, 627–637 (2006).
25. H. Y. Ryu, H. S. Moon, and H. S. Suh, "Optical frequency comb generator based on actively mode-locked fiber ring laser using an acousto-optic modulator with injection-seeding," *Opt. Express* **25**, 11396–11401 (2007).
26. M. Nikodem and K. Abramski, "Controlling the frequency of the frequency shifted feedback fiber laser using injection-seeding technique," *Opt. Commun.* **283**, 2202–2205 (2010).
27. M. V. Berry and S. Klein, "Integer, fractional and fractal Talbot effects," *J. Mod. Opt.* **43**, 2139–2164 (1996).

1. Introduction

Frequency shifted feedback (FSF) lasers have attracted a sustained attention during the last 25 years because of their counter-intuitive physical properties that have triggered a large amount of fundamental studies in laser dynamics [1] or optical coherence [2–4], and have found applications in very diverse areas: communications protocols [5], atomic physics [6], telemetry [7], profilometry [8] and sensing among others. Recall that a FSF laser is a laser cavity closed on the +1 (or -1) diffraction order of an acousto-optics frequency shifter (AOFS): each time a photon makes a roundtrip in the cavity its frequency is increased (or decreased) by the AOFS frequency in the case of a ring cavity, and by twice this frequency in the case of a linear cavity. The process is repeated over successive roundtrips of the light field in the cavity, which confers to this laser source an intrinsic chirp and peculiar time-frequency properties [3].

A FSF laser can operate with or without external seeding. When seeded only with spontaneous emission FSF lasers can exhibit different regimes, depending essentially on the influence of the gain dynamics and non-linear effects like cross-phase modulation. When the influence of the gain medium and possible non-linear effects are neglected as in the passive cavity model, the output optical field shows a modeless spectrum and consists, in the time-frequency representation, in a periodic function chirping with time [9, 10]. In the case where the frequency shift per roundtrip is much smaller than the cavity free spectral range, the periodic function tends to a Dirac comb and the FSF laser field can be seen as a frequency comb chirping in the time-frequency plane [11]. On the contrary when the gain dynamics and non-linear effects cannot be neglected, various pulsing regimes have been reported in the literature so far [12], especially in fiber FSF lasers where the spatial confinement enhances the non-linear effects [13–18].

The case where the FSF cavity is seeded with a monochromatic field has been partially investigated in early work on FSF lasers. Kowalski reported first the possibility to generate pulses from a passive FSF cavity seeded with a CW He-Ne laser, when the frequency shift per roundtrip f_s was equal to the cavity free spectral range f_c [19]. Then the same team observed numerically in the frame of the passive cavity model, that when the two frequencies are in the ratio $f_s/f_c = p/q$ (p and q being coprime integers) the laser generates pulses at repetition rate qf_s [20]. An experimental demonstration was given in 1993 in the case $f_s/f_c = 2$ [21]. Meanwhile the application of this system as an optical synthesizer had been proposed [22]. In 2004 Yatsenko *et al.* developed a numerical model of a FSF laser where the gain and losses of the cavity were taken into account, which proved numerically the possibility of increasing the repetition rate by adjusting the frequency shift f_s and the cavity free spectral range f_c as the ratio of two integers [23]: in this case, supposing $f_s/f_c = p/q$, the repetition rate is equal to $qf_s = pf_c$. Since then however, despite recent experimental investigations of seeded FSF lasers for frequency combs and metrology applications [24–26], to our knowledge no experimental evidence of the multiplication of repetition rates in CW injection seeded FSF cavities has been reported, beyond the case $f_s/f_c = 2$.

In this paper we develop a brief analytical explanation of this effect and report an experimental demonstration of the generation of ultrahigh and tunable repetition rates in CW-seeded FSF lasers for values of p and q as large as 183 and 586 respectively. Indeed we prove the generation of 6 ps Fourier-transform limited pulses with a repetition rate tunable by steps of $f_s = 80$ MHz between $3 \times f_s$ (240 MHz) and $458 \times f_s$ (37 GHz), with an average power larger than 100 mW. We provide a simple (linear) model based on the interference of the optical modes of the frequency comb generated at the output of the CW injection-seeded FSF laser, and attribute this behavior to the fact that the phase of the n^{th} mode has a quadratic dependence with n .

We expect this demonstration to have significant outcomes for the implementation of lasers with GHz to THz repetition rates.

2. Theoretical description

2.1. Expression of the electric field

First we provide a brief analytical description of the generation of Fourier-transform limited pulses with ultrahigh repetition rates in CW injection-seeded FSF lasers. For simplicity reasons we neglect the self-seeding of the cavity with spontaneous emission. (Note however that a more realistic description would require involving the spontaneous emission, since it is predicted to play a non-negligible role in the behavior of the FSF laser [3]). We consider a FSF cavity characterized by the roundtrip time $\tau_c = 1/f_c = 2\pi/\omega_c$ and the frequency shift per roundtrip $f_s = \omega_s/2\pi$ (Fig. 1). The cavity is seeded continuously with a monochromatic field $E_0 e^{-i\omega_0 t}$: at each roundtrip in the cavity the angular frequency is shifted by ω_s . A slightly transmitting mirror enables to extract a fraction of the intracavity field. The output optical spectrum consists in a comb of optical modes separated by the frequency f_s . The influence of the gain and losses of the FSF cavity is modeled by a real and positive function g , where $E_0 g(n)$ is the amplitude of the mode of angular frequency $\omega_0 + n\omega_s$. One sets $g(n) = 0$ when $n < 0$ and $n > N$, the cutoff limit of g (Fig. 1). Calling $\Delta\omega$ the spectral bandwidth of the FSF laser, $N = \Delta\omega/\omega_s$. The electric field at the output of the cavity is, following [19, 20, 23]:

$$E(t) = E_0 [g(0)e^{-i\omega_0 t} + g(1)e^{-i(\omega_0 + \omega_s)t + i\phi_1} + g(2)e^{-i(\omega_0 + 2\omega_s)t + i\phi_2} + g(3)e^{-i(\omega_0 + 3\omega_s)t + i\phi_3} + \dots] \quad (1)$$

where $\phi_1 = (\omega_0 + \omega_s)\tau_c$, $\phi_2 = \phi_1 + (\omega_0 + 2\omega_s)\tau_c$, $\phi_3 = \phi_2 + (\omega_0 + 3\omega_s)\tau_c$... Finally the phase

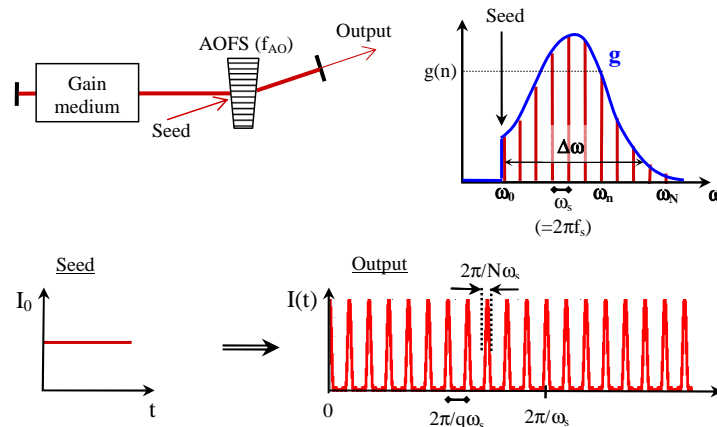


Fig. 1. Top left: sketch of a generic (linear) FSF laser. The FSF cavity is injected through a leak of the AOFs. The AOFs is driven at frequency f_{AO} . The laser mode is diffracted by the traveling acoustic wave onto the +1 order and frequency-shifted by f_{AO} , resulting in a frequency shift per roundtrip equal to $f_s = \omega_s/2\pi = 2f_{AO}$. The cavity roundtrip time is $\tau_c = 1/f_c$. Top right: optical spectrum of the output of the FSF laser seeded by a monochromatic wave at angular frequency ω_0 . The envelope of the spectrum of the FSF frequency comb is the function g (see text). Bottom: when $f_s/f_c = p/q$ the FSF cavity transforms a CW seed laser field into a pulsed one with a repetition rate equal to qf_s (see text).

of the n^{th} mode is: $\phi_n = n\omega_0\tau_c + n(n+1)\omega_s\tau_c/2$ and the resulting electric field is:

$$E(t) = E_0 e^{-i\omega_0 t} \sum_n g(n) e^{-in\omega_s t} e^{in\omega_0\tau_c} e^{i\frac{n(n+1)}{2}\phi} \quad (2)$$

where $\phi = \omega_s\tau_c = 2\pi f_s/f_c$. Note that $E(t)$ appears as a Fourier series with phase terms quadratic in n : the same kind of expression was previously shown as playing a fundamental role in the time-spectrum description of modeless FSF lasers [9, 10]. In the following it is shown that these quadratic phases play also a decisive role in the expression of the intensity at the output of the CW injection-seeded FSF laser.

2.2. Expression of the intensity

The intensity of the laser field is $I(t) = E(t)E^*(t)$. Writing $I_0 = |E_0|^2$ leads to:

$$I(t) = I_0 \sum_{n,m} g(n)g(m) e^{-i(n-m)(\omega_s t - \omega_0\tau_c - m\phi)} e^{i\frac{(n-m)(n-m+1)}{2}\phi} \quad (3)$$

which can be rewritten as (introducing $k = n - m$):

$$I(t) = I_0 \sum_k e^{-ik(\omega_s t - \omega_0\tau_c)} e^{i\frac{k(k+1)}{2}\phi} \sum_m g(k+m)g(m) e^{-ikm\phi}. \quad (4)$$

The occurrence of the sum $\sum_m g(k+m)g(m) e^{-ikm\phi}$ is a direct consequence of the quadratic phases in Eq. (2): it ensures a selection of specific values of k based on the comparison between the width of the function $m \mapsto g(k+m)g(m)$ and the period of $m \mapsto e^{-ikm\phi}$. For simplicity reasons it is assumed $g(m)$ is a Gaussian function of characteristic width $N/2$. Then the width of $g(k+m)g(m)$ is $N/2\sqrt{2}$. For integers k satisfying:

$$-\frac{2\sqrt{2}}{N} < k\phi [2\pi] < \frac{2\sqrt{2}}{N} \quad (5)$$

the term $\sum_m g(k+m)g(m)e^{-ikm\phi}$ is a sum of positive terms whereas for other values of k , both positive and negative terms appear in the sum and limit its amplitude. Therefore only integers satisfying Eq. (5) contribute significantly to the sum over k arising in Eq. (4). We consider the case $\phi = 2\pi p/q$ where p and q are coprime integers and $q < N$. Then the previous condition reduces to: $-\frac{\sqrt{2}}{\pi} \frac{q}{N} < pk [q] < \frac{\sqrt{2}}{\pi} \frac{q}{N}$. Since pk is an integer and $\frac{\sqrt{2}}{\pi} \frac{q}{N} < 1$, it sets $k = 0 [q]$. Then the intensity rewrites:

$$I(t) = I_0 \sum_k G(kq) e^{-ikq(\omega_s t - \omega_0 \tau_c)} e^{i\pi p k(kq+1)} \quad (6)$$

where $G(\lambda) = \sum_m g(\lambda+m)g(m)$ is the discrete autocorrelation function of g . Assuming that p is even or q is odd:

$$I(t) = I_0 \sum_k G(kq) e^{-ikq(\omega_s t - \omega_0 \tau_c)} \quad (7)$$

whereas when p is odd and q is even,

$$I(t) = I_0 \sum_k G(kq) (-1)^k e^{-ikq(\omega_s t - \omega_0 \tau_c)}. \quad (8)$$

In both cases since $G(\lambda)$ is real this Fourier series describes Fourier transform-limited pulses at the repetition rate $qf_s = pf_c$, according to $\phi = 2\pi f_s/f_c = 2\pi p/q$ [23]. The time duration of the pulses is limited by the spectral bandwidth of the intensity spectrum and scales therefore as $2\pi/(N\omega_s) = 2\pi/\Delta\omega$. The average intensity is constant and equal to $\bar{I} = I_0 G(0)$ whereas the peak intensity is equal to $I_{peak} = I_0 \sum_k G(kq)$. The conservation of energy leads to $I_{peak} \approx I_0 G(0) N f_s/q$. Note that the maximal repetition rate is limited by the number of modes and therefore by the spectral bandwidth of the laser: when q becomes comparable to N , the pulses begin to overlap.

The notable consequence of this calculation is the fact that a CW injection-seeded FSF laser is a source of Fourier-transform-limited pulses with a tunable repetition rate: the latter can be adjusted simply by varying the ratio p/q , *i.e.* f_s or f_c . It is also interesting to compare this expression to that of the intensity delivered by a mode locked laser with a frequency spacing $f_s = \omega_s/2\pi$ and having the same optical spectrum but constant phases. In this case the expression of the intensity is quite similar:

$$I_{ML}(t) = I_0 \sum_k G(k) e^{-ik\omega_s t} \quad (9)$$

and corresponds to Fourier-transform pulses at the repetition rate f_s . Remarkably both laser fields share the same optical spectrum and deliver the same average intensity, but exhibit a different intensity spectrum. The multiplication of the repetition rate in a CW injection-seeded FSF laser results from a decimation in the intensity spectrum, *i.e.* from the selection of spectral components multiples of $q\omega_s$ which is a direct effect of the quadratic phases arising in the expression of the electric field.

2.3. Intensity fluctuations

When $\phi = 2\pi p/q$, the laser emits pulses at the repetition rate qf_s and a signature of this appears in the variation with ϕ of the relative intensity fluctuations of the laser defined by:

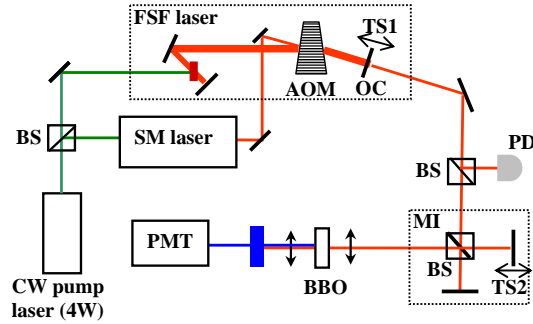


Fig. 2. Experimental setup to characterize the pulsing output and the intensity fluctuations of the seeded FSF laser. AOM is the acousto-optics frequency shifter, SM denotes the seeding single mode laser, BS is a beamsplitter, PD and PMT are respectively the fast photodiode and the photomultiplier tube, TS1 and TS2 are translation stages and MI stands for Michelson interferometer. OC is the output coupler of the FSF laser.

$$W(\phi) = \frac{\langle I^2(t) \rangle}{\langle I(t) \rangle^2}(\phi) \quad (10)$$

where $\langle \rangle$ denotes the average over time. When $\phi = 2\pi p/q$ with $q \ll N$, the laser emits q pulses per period $2\pi/\omega_s$. The average intensity does not depend on the repetition rate and a simple calculation leads to: $W(2\pi p/q) \sim 1/q$. The intensity fluctuations of the injected FSF laser tend therefore to the self-similar so-called "Thomae's function" defined on $[0, 1]$ by: $T(p/q) = 1/q$ when p and q are coprimes, and $T(\eta) = 0$ when η is irrational.

3. Experimental validation

3.1. Experimental setup

To validate this brief description of the seeded FSF laser, we demonstrated the possibility of high repetition rates in a dye FSF laser seeded by a single-mode stabilized dye laser (Coherent 599) with a typical linewidth of 1 MHz. Both lasers are pumped by a 4 W CW pump laser at 532 nm whose intensity is equally distributed between both lasers (Fig. 2). The single mode laser delivers about 30 mW at 580 nm and injects the FSF laser via the zero diffraction order of AOFs. The insertion losses are about 90%. The FSF laser consists in a linear cavity closed on the +1 diffraction order of the AOFs. The latter is driven at the (fixed) frequency 40 MHz, which leads to a frequency shift per roundtrip $f_s = 80$ MHz. The output coupler of the FSF laser is mounted on a translation stage (TS1) enabling to scan the cavity length over more than 7 cm and consequently the cavity free spectral range f_c between 240 and 280 MHz. The typical output beam power is 100 mW and the spectral bandwidth is 150 GHz. The latter can be reduced down to about 3 GHz by the insertion in the FSF cavity of a Fabry-Perot etalon. A fraction of the output beam is directed onto a fast photodiode (100 ps resp. time) and the signal is acquired by a fast digital oscilloscope (5 GHz BW). The other part of the beam is sent into a Michelson interferometer whose moving mirror is mounted on a second translation stage (TS2). The output of the interferometer is focused onto a BBO crystal tuned for second harmonic generation (SHG) at 580 nm. The UV signal is filtered out by a prism and a color glass plate and detected by a photomultiplier tube (PMT).

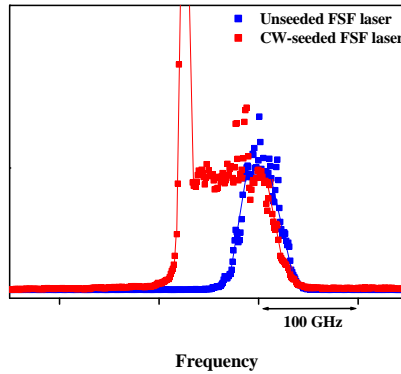


Fig. 3. Optical spectrum of the FSF laser with and without injection. The frequency of the injection laser corresponds to the large peak on the left wing on the spectrum.

3.2. Experimental results

First we characterize the optical spectrum without and with injection (Fig. 3). Without injection the (modeless) spectrum is found to be 60 GHz wide. To minimize the effects of spontaneous emission and avoid the so-called modeless regime, the frequency of the seed laser is adjusted about 100 GHz below the maximum of the modeless spectrum: the resulting spectrum is then shifted to the low frequencies and spans over 150 GHz.

We now investigate the cases where $\phi = 2\pi p/q$, that is f_s/f_c is a rational quantity. f_s is kept constant while f_c is adjusted by tuning the cavity length with TS1. First the cavity length is adjusted to relatively low values of q ($q < 30$) and the intensity spectrum of the FSF laser is recorded for different values of the cavity free spectral range. Results are plotted on Fig. 4 and demonstrate the decimation in the intensity spectrum predicted theoretically: beside additional beat notes of smaller amplitude, only RF frequencies corresponding to common multiples of f_s and f_c appear in the intensity spectrum, in accordance to Eq. (6). This also corresponds to the fact that the repetition rate of the laser is the least common multiple of f_s and f_c .

Second to investigate large values of q (which corresponds to repetition rates out of reach of our electronic detection system) we record the interferometric autocorrelation trace $\langle |E(t) + E(t + \tau)|^4 \rangle$ by measuring the time-averaged SHG signal at the output of the interferometer (τ is the time delay of the interferometer). The cavity length is adjusted to a given value $f_c = (q/p)f_s$ and the mobile arm in the Michelson interferometer is scanned around null delay by TS2. A central fringe pattern is recorded in all cases, independently from the cavity length and represents the autocorrelation of a single pulse (Fig. 5). Note that the width of this trace is independent from the cavity length and simply proportional to the inverse of the spectral bandwidth of the laser, that is the coherence time of the source. In the case of a pulsed source the theoretical ratio between the baseline and the top of the fringes is equal to 1:8. A slightly lower value is obtained in our case due to an average over the fringes caused by the excessive scan speed of TS2. The appearance of additional peaks in the autocorrelation trace for path delays much smaller than the cavity length is the signature of the multiplication of the repetition rate and corresponds to the overlap of successive light pulses at the output of the interferometer. It could be shown theoretically that the lack of fringe pattern in the satellite peaks is due to the absence of average coherence between consecutive pulses, which results in the 1:2 ratio between the baseline and the height of the secondary peak. The repetition rate can be deduced from the time delay between consecutive peaks on the autocorrelation trace while the pulse

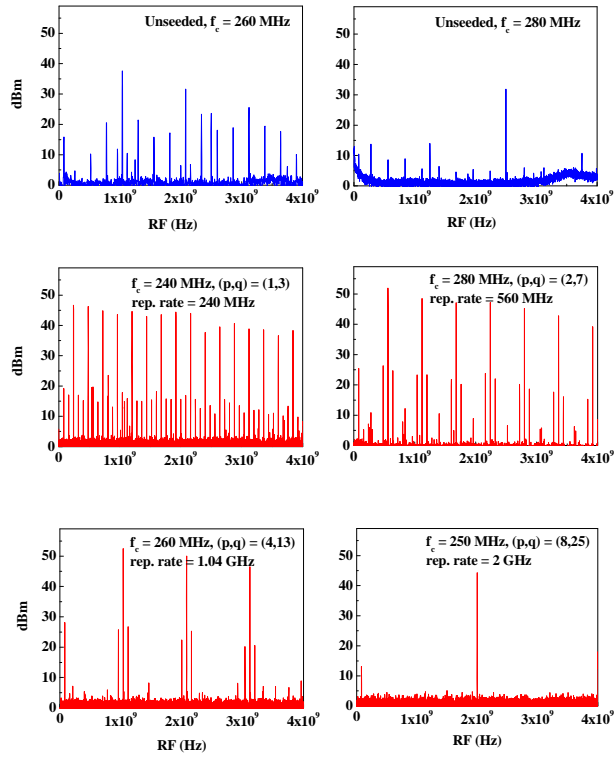


Fig. 4. Intensity spectra of the seeded FSF laser recorded for different values of the cavity free spectral range. f_s is kept equal to 80 MHz. Top left and top right: for comparison, intensity spectrum of the FSF laser without injection ("modeless" regime). Center and bottom plots: intensity spectra of the CW injection-seeded FSF laser for different values of f_c . f_s/f_c is set as the ratio of two coprime integers p/q . The principal beat notes correspond to common multiples of f_s and f_c .

duration corresponds to the widths of the peaks. According to the theoretical description, Fig. 5(b) evidences the generation of 6 ps duration Fourier-transform limited pulses at a repetition rate as high as 37 GHz, which is close to the ultimate limit set by the bandwidth of the laser (150 GHz in this case).

Finally we measure the variation of the intensity fluctuations with the cavity length. The moving arm of the interferometer is blocked and the time-averaged SHG signal \bar{I}_ϕ^{SHG} is recorded as a function of the cavity length by scanning TS1 continuously. Since $\bar{I}_\phi^{SHG} \propto \langle I^2(t) \rangle(\phi)$, it is proportional to the intensity fluctuations of the seeded FSF laser $W(\phi)$. The experimental results are shown on Fig. 6. When the spectral bandwidth of the laser is increased from 3 to 150 GHz, the intensity fluctuations tend to the self-similar Thomae's function and reveal self-similarity.

4. Conclusion

We have demonstrated that a FSF laser seeded with a monochromatic laser is a source of Fourier-transform limited pulses at a tunable (and possibly ultra-high) repetition rate. The max-

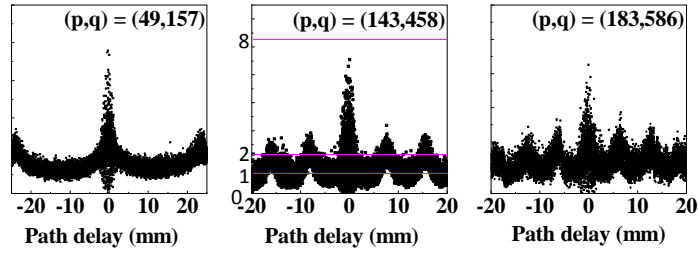


Fig. 5. Interferometric autocorrelation traces recorded for different values of (p, q) . By adjusting the position of the output coupler (TS2), the cavity free spectral range is tuned to 256.33 MHz, 256.22 MHz and 256.17 MHz from left to right and the repetition rates are 12.56 GHz, 36.64 GHz and 46.88 GHz respectively. The time duration of the peaks is about 6 ps, corresponding to the inverse of the spectral bandwidth of the laser (150 GHz).

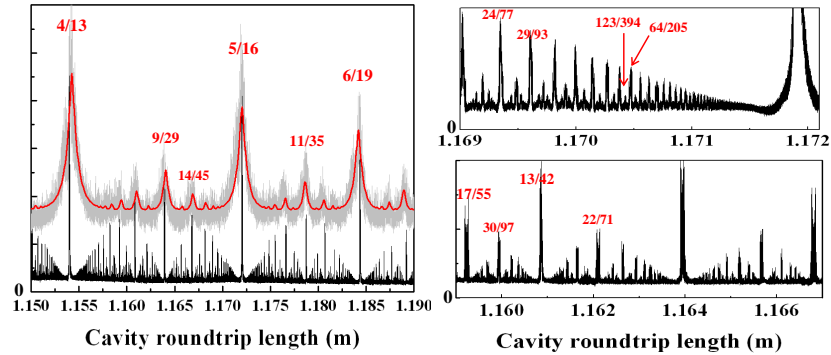


Fig. 6. Intensity fluctuations of the seeded FSF laser with the cavity length measured by SHG (linear scale). The spectral bandwidth of the laser is equal to about 3 GHz (grey plot, shifted vertically for clarity) or 150 GHz (black plots). The red curve is a theoretical plot taking into account a spectral profile defined as $g(n) = 0.975^n$ corresponding to a spectral bandwidth of $\Delta\omega = -\omega_s / \ln(0.975)$ equal to 3 GHz. The peaks are labeled by the corresponding value of p/q (in red).

imum repetition rate of the laser is limited by the temporal overlap of consecutive optical pulses, *i.e.* by the spectral bandwidth of the laser. We have given a brief analytical description of this phenomenon, based on a linear approach, *i.e.* a pure interference phenomenon between waves with quadratic phases, ignoring both dynamic or non-linear effects. This simple approach is sufficient however to account for the experimental results. In the present study the repetition rate is a multiple of $f_s = 80$ MHz and tunable over two orders of magnitude between $3 \times f_s$ and $458 \times f_s$. Note that we have neglected so far the role of the coherence of the seed laser since our theoretical description involves a pure monochromatic wave. In fact to ensure Fourier transform-limited pulses, the coherence time of the seed laser needs to be longer than the photon cavity lifetime in the cavity, that is $N\tau_c$. In the current experiment the coherence time of the seed laser ($1 \mu\text{s}$) is of the same order of magnitude (although smaller) as the photon cavity lifetime (about $4 \mu\text{s}$). To demonstrate ultrahigh repetition rates (100 GHz to THz), seed lasers with longer coherence time will be required, such as extended-cavity diode lasers or distributed feedback lasers (with $10 \mu\text{s}$ up to 1ms respective coherence times). Finally an additional advantage of this scheme for high repetition rates is the fact that the repetition rate is derived from the electronic frequency driving the AOFS, and not only from the cavity free spectral range, like in conventional passive mode-locking.

This work constitutes a proof of principle promising for various applications where ultrahigh repetition rate lasers are necessary: ultrafast digital communications and optoelectronics processing systems, THz generation, spectroscopy of metallic nanoparticles. The requirements related to ultra-high repetition rates, the influence of the line width of the seed laser, the limitations of the spectral purity of the repetition rate, the link with the fractional Talbot effect [27] and the role of spontaneous emission, intracavity dispersion and nonlinear effects in the FSF cavity will be addressed in detail in forthcoming publications.

5. Acknowledgments

This work was supported in part by the CNRS and the LIPhy. J. M. was supported by the the Royal Society, the Leverhulme Trust and ERC. We acknowledge D. Comparat for the realization of the single-mode laser, and the referees for their contribution to the improvement of the manuscript.